Advances in Reliability, Safety and Security, Part 9 – Kołowrocki, Dąbrowska (eds.)
 ISBN 978-83-68136-21-0 (printed), ISBN 978-83-68136-08-1 (electronic)

Advances in Reliability, Safety and Security

ESREL 2024
Monograph Book Series

Method Of Constructing Data Fusion Spatio-Temporal Graph Of Truss Bridge Fracture Based On Vibration Signals

Meng Li, Yanxue Wang, Xinming Li

School of Mechanical-Electronic and Vehicle Engineering, Beijing University of Civil Engineering and Architecture, Beijing,100044, China

Abstract

To improve bridge structural health monitoring (SHM) accuracy and efficiency, this paper proposes an algorithm for constructing a spatio-temporal graph based on vibration signal fusion of truss bridge fracture data. First, a cross-edge weight standard deviation (C-EWSD) feature is proposed to fuse the multi-channel sensor spatio-temporal data. Then, the C-EWSD features are combined with the time-frequency features to extract the node spatio-temporal features. The truss bridge node spatio-temporal graph signal is established according to the spatio-temporal characteristics and the spatial node topology graph. Determine the bridge structure warning position from the node offset on the spatio-temporal graph. The experimental results show that the proposed algorithm can effectively judge the faults and put forward the early warning on the truss bridge fracture diagnosis, which has a good engineering application prospect.

Keywords: spatio-temporal graph, structural health monitoring, signal processing, truss bridge, fracture diagnosis

1. Introduction

Given that structural health monitoring (SHM) of bridges is crucial for urban transport and people's lives, bridge health diagnostics based on vibration signals are of great significance in engineering. With the development of intelligent sensors, communication technology, and intelligent algorithms, the continuous monitoring process of the dynamic response of civil engineering and buildings has become possible. Big data processing technology in the structural health monitoring process and data science and engineering technology in the computer field have been extensively studied and applied to dynamic monitoring of civil engineering structures (Delgadillo and Casas, 2019; Kim et al., 2013). For example, the data collection algorithms based on compressed sampling (Bao et al., 2011, 2018), the abnormal data diagnosis methods using deep learning algorithms (Xu et al., 2018), the crack identification methods using computer vision technology (Fischer and Igel, 2010; Liu et al., 2017; Xu et al., 2019), and bridge health assessment using machine learning algorithms (Delgadillo and Casas, 2019; Li et al., 2018; Wei et al., 2017) and other methods. However, monitoring and analyzing the entire building group or composite structure using traditional single-point sampling analysis is difficult. Therefore, new theories need to be introduced to establish a system-level structural health monitoring system.

Graph Signal Processing (GSP) is a new signal processing framework in irregular domains that extends from discrete signal analysis (Sandryhaila and Moura, 2013, 2014). GSP can extend single-point time series signal to multi-element information fusion analysis and can judge the health status of equipment operation comprehensively (Liu and Wang, 2001). The spatio-temporal graph is a new signal processing framework based on non-sparse dictionary representation and uses edges to describe the correlation of signals (Mei and Moura, 2016; Ortega et al., 2018). SHM based on spatio-temporal signals is an important research field with wide applications in engineering, construction, aerospace and other fields. Scholars have done a lot of research in the field of SHM based on spatio-temporal signals. In constructing and predicting sustainable urban development, Zhang et al. (2023) proposed spatio-temporal graph learning based on adversarial adaptivity for modeling urban sensing systems. Zhou et al. (2024) introduced complementary spatio-temporal learning based on hints of

ComS2T for augmenting the evolution of data-adaptive models. In the field of mechanical fault diagnosis, Song et al. (2022) developed a spatio-temporal neural network (STN) model for fault diagnosis of bearings, which is constructed by a multilayer fusion of long-term memory network features and a Convolutional Neural Network (CNN). To accurately predict the flow state prediction of gas-water two-phase, Li et al. proposed a method of extracting spatio-temporal signatures of the process from multimodal measurement signals, which visually indicates the transition state by quantifying the long-term waveform variations of the state signatures and equilibrium relationships (Li et al., 2023). Spatio-temporal signal structural health monitoring aims to monitor and analyze signals inside structures in real-time. This method helps to detect possible structural defects, damage and failures in advance. Then take corresponding maintenance or reinforcement measures to ensure the safe and reliable operation of the structure. However, there are few studies in the spatio-temporal area in bridge structure health monitoring.

The truss bridge is a multi-node statically indeterminate structure. During operation, the bridge will be affected by vehicle, ground, and wind loads, so data monitoring in time and space is necessary for bridge health monitoring. Single sensor data information is difficult to accurately reflect the health status of the truss, we proposed a truss bridge fracture diagnosis algorithm based on spatio-temporal graph signals. The main contributions of this article are listed as follows:

(1) We propose a spatio-temporal graph construction algorithm for truss bridges. Combining the efficient multi-sensor system and the bridge structure, a data fusion spatio-temporal graph model based on bridge spatial nodes and digital signals was established, which can intuitively reflect the node-to-node relationship on the graph and enhance the degree of data visualization;

(2) We propose a signal contrast feature of cross-edge weight standard deviation (C-EWSD). C-EWSD reflects the correlation and change of node-to-node relationship in the time dimension, spatial dimension and different health status conditions. C-EWSD features are combined with time-frequency features for data enhancement to obtain fusion coefficients to reflect the correlation between nodes;

(3) We constructed a truss bridge fracture diagnosis model based on vibration signals. The correlation changes between nodes on the spatio-temporal graph can reflect the health status of the bridge, and visual warning information is provided for the damage location.

2. Theory

To establish the spatio-temporal relationship between bridge nodes, we propose a spatio-temporal graph construction algorithm based on multi-channel vibration signals. The algorithm flow is shown in Figure 1.

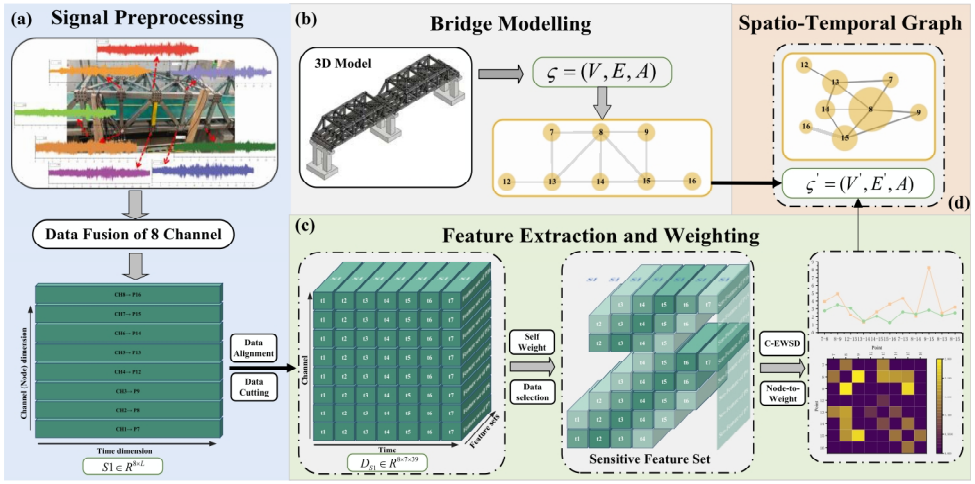

Fig. 1. The flowchart of the proposed method:
(a) **Signal processing**: Measure 8-channel vibration data from the experimental bridge and perform data alignment and cutting;
(b) **Bridge modeling**: Establish a 3D model of the bridge, mark nodes, and establish node spatial relationships;
(c) **Feature extraction and weighting**: Select 5 sensitive features from 39 time-frequency features, intercept the main signal components, and calculate the correlation coefficients between nodes based on the **C-EWSD features**;
(d) **Spatio-temporal graph**: Generate spatiotemporal graph signals based on correlation coefficients and spatial relationships between nodes.

The algorithm is based on the proposed C-EWSD metrics combined with the time-frequency domain metrics to establish the correlation coefficients between nodes. The node-to-node distance on the graph is updated based on the node spatial and correlation coefficient, and a spatio-temporal graph signal that can provide early warning of damage is established. Specifically, the algorithm integrates the spatial nodes of the bridge and the time-series vibration signal of the entire process of vehicles passing through the bridge. First, we built the bridge's spatial relationship through 3D modeling and a complete experimental device. Secondly, in the vehicle-bridge joint experiment, we collected the vibration signals of multiple nodes at the same time to establish the spatio-temporal relationship: in the time dimension, the time series signal of the vehicle passing through the bridge was collected from each node; in the spatial dimension, we obtain the vibration signal of each node at the same time point or same time interval. The spatial dimension and the time dimension can enhance each other's relation to establish the correlation between nodes more accurately. The correlation is a fusion correlation of time series vibration signals based on spatio-networks. We collected continuous data from vehicles passing through nodes equipped with sensors on the bridge. The signal of vehicles passing through different nodes in different time intervals through data interception established a strong correlation between nodes from the spatio-temporal perspective.

2.1. Signal processing

In this experimental bridge, 29 nodes were labeled for marking and installing sensors, as shown in Figure 2(a). The start and stop of data collection are controlled manually, so there is a null-acquisition time at the beginning and end of the detected data (that is, the time gap between data collection instrument collection and vehicle operation). The original data must be aligned and segmented to obtain data collected from different nodes at different time intervals. As shown in Figure 2(b), this paper divides the bridge truss segment according to the node distribution. It divides the bridge into 7 segments, each corresponding to different time and spatial nodes. Take the data S_2 of 8-14 main truss fractures as an example. S_2 contains 8-channel data of length L. After repeated experiments, the vehicle running time $T_2 = 20.8s$ when speed is $0.1m/s$. This paper designs a null-acquisition time calculation algorithm to intercept valid data. There is a large energy difference between the connection section of the static signal and the operating signals' connection section. Removing the null-acquisition time can get the optimal signal period.

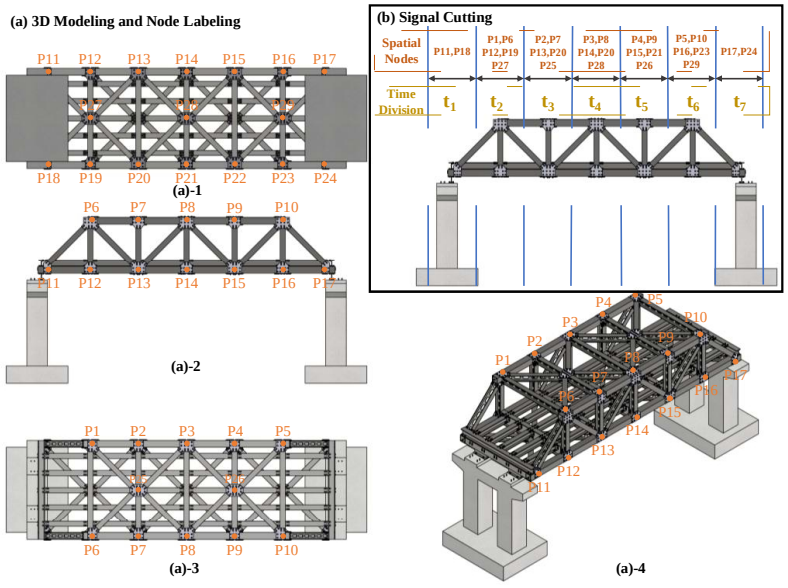

Fig. 2. Bridge 3D modeling and signal segmentation basis.

First, the energy changes at the start and stop moments, the moving average partial energy value method is used to calculate the null-acquisition time ΔT_i at the beginning. The signal after the vehicle starts and the signal before it stops have higher energy values due to vehicle movement. Therefore, the data with a length of ΔL at the

starting and end are intercepted respectively. The upper envelope signal is used as an energy measure to calculate the upper envelope average $E(t_1)$:

$$E(t_1) = \frac{\sum_1^L \mathfrak{E}(S_2(t_1, t_1+\Delta L/fs)) + \sum_1^L \mathfrak{E}(S_2(t_1+T_2-\Delta L/fs, t_1+T_2))}{2} \quad (1)$$

where $\mathfrak{E}()$ is the envelope calculation and t_1 is the moving average start.

If the two segments of the intercepted signal include the null-acquisition time, $E(t_1)$ is lower than $E(t_1)$ of the signal at vehicle movement, so t_1 is the starting time corresponding to when $E(t_1)$ is the largest, which is the starting null-acquisition time ΔT_i:

$$\Delta T_i = \{t1 | \max\ \mathrm{E}(t_1), t_1 = 0{,}0.01 * \Delta L/fs, 0.02 * \Delta L/fs, \cdots, L_i/fs - T_2\} \quad (2)$$

where the length of each move interval of t_1 is $0.01 * \Delta L/f_s$ and $f_s = 12.8kHz$ is the sampling frequency. The new data set excluding the null-acquisition time is $S_2' \in R^{8\times L_s}$, where $L_s = f_s * T_2$.

The distance between the vehicle and the sensor impacts the signal. We discarded the data whose vehicles were far from the sensor for dimensionality reduction. As shown in Figure 1, only the data segments collected when the vehicle passes through this node and adjacent nodes are retained. When a vehicle passes through a node, the signal segments captured by the sensors on the node are defined as the primary signals and the signal segments captured by the sensors arranged in the neighboring nodes are defined as the secondary signals for that node.

2.2. Cross-edge weight standard deviation calculation

To extract the spatio-temporal correlation between nodes, this paper creatively proposes the cross-edge weight standard deviation (C-EDSW) feature extraction algorithm, as shown in Figure 3. In this paper, the vehicle is the motion excitation source, and the excitation points are the four wheels of the vehicle, which produce signal features possessing a correlation with the motion path. The C-EDSW between nodes is a feature based on the signal waveform and energy. The nodes of the truss bridge are connected similarly and the physical connection between neighboring nodes is transmissible. We make two assumptions: a. When the vehicle passes a fixed distance before and after each node, the signal collected by the sensors arranged at the node are similar; b. The signals collected by the sensors at the neighboring nodes are highly similar because of the transmissibility of the physical connection.

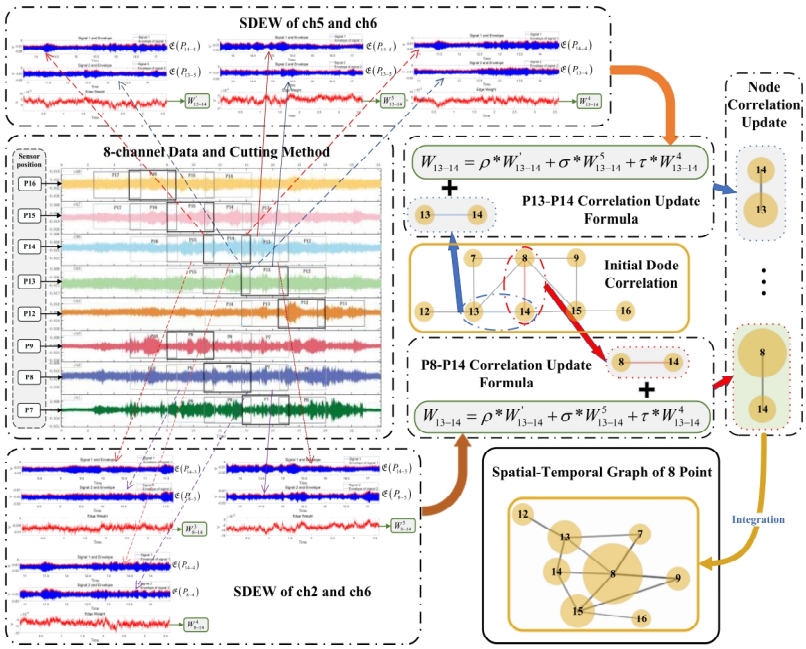

Fig 3. The flowchart of the proposed C-EDSW method.

Based on the spatial relationship of the bridge, we define the nodes with spatial connection as associated node pairs, which means the two nodes have a neighboring relationship, such as node P7 and node P8, nodes P8 and node P14. It is easy to see that all node pairs are in the same time interval or adjacent time intervals. Therefore, we calculate the association relationship between nodes P_a and P_b in two cases, i.e., the two nodes are in the same or adjacent time intervals.

(1) Nodes P_a and P_b are in same time interval

CH_a and CH_b are the complete signals collected by the sensors deployed on nodes P_a and P_b. The corresponding time interval where nodes P_a and P_b are located is t_j. There are 6 data segments used to calculate the node relationship, as shown the C-EWSD of ch2 and ch6 in Figure 3. The envelope is calculated by moving window local maximum method:

$$\begin{cases} \mathfrak{E}(P_{a-j})(k) = \max\left(CH_{a-j}(k, k+\Delta l)\right) \\ \mathfrak{E}(P_{a-j-1})(k) = \max\left(CH_{a-j-1}(k, k+\Delta l)\right) \\ \mathfrak{E}(P_{a-j+1})(k) = \max\left(CH_{a-j+1}(k, k+\Delta l)\right) \\ \mathfrak{E}(P_{b-j})(k) = \max\left(CH_{b}(k, k+\Delta l)\right) \\ \mathfrak{E}(P_{b-j-1})(k) = \max\left(CH_{b-j-1}(k, k+\Delta l)\right) \\ \mathfrak{E}(P_{b-j+1})(k) = \max\left(CH_{b-j+1}(k, k+\Delta l)\right) \end{cases}, \quad k = 1,2,\cdots, L_1 - \Delta l \tag{3}$$

where CH_{a-j} is the data segment corresponding to time interval t_j of the signal collected by the sensor Channel (a) on P_a (i.e., the data CH_{a-j} is the signal when the vehicle passes through P_a), $\mathfrak{E}(P_{a-j})$ is the envelope of CH_{a-j}, L_1 is the length of CH_{a-j}, and Δl is the sliding window width of the envelope.

When nodes P_a and P_b are in the same time interval, the C-EWSD between P_a and P_b is defined as the standard deviation of edge weight (EWSD) of two-channel data on the same time interval when the vehicle passes through the two nodes and the neighboring nodes, i.e., the SDEW of the data on the time interval t_j, t_{j-1} and t_{j+1}:

$$W_{a-b}^{j} = \frac{1}{L_1 - \Delta l}\sum_{1}^{L_1-\Delta n}\left|\mathfrak{E}(P_{a-j}) - \mathfrak{E}(P_{b-j})\right| \tag{4}$$

$$W_{a-b}^{j-1} = \frac{1}{L_1 - \Delta l}\sum_{1}^{L_1-\Delta n}\left|\mathfrak{E}(P_{a-j-1}) - \mathfrak{E}(P_{b-j-1})\right| \tag{5}$$

$$W_{a-b}^{j+1} = \frac{1}{L_1 - \Delta l}\sum_{1}^{L_1-\Delta n}\left|\mathfrak{E}(P_{a-j+1}) - \mathfrak{E}(P_{b-j+1})\right| \tag{6}$$

The C-EWSD between nodes P_a and P_b in the same time interval is defined as:

$$W_{a-b} = \rho * W_{a-b}^{j} + \sigma * W_{a-b}^{j-1} + \tau * W_{a-b}^{j+1} \tag{7}$$

where $\rho + \sigma + \tau = 1, \rho \geq 0.5$, the three parameters are dynamically adjusted according to the training results.

(2) Nodes P_a and P_b are in adjacent time intervals

When P_a and P_b are in adjacent time intervals: t_j and t_{j+1}. As shown the C-EWSD of ch2 and ch6 in Figure 3, there are four signal segments in the two node channels used to calculate C-EWSD of P_a and P_b : $CH_{a-j}, CH_{b-j}, CH_{a-j+1}, CH_{b-j+1}$ from sensors on P_a and P_b corresponding to t_j and t_{j+1}, respectively.

$$\begin{cases} \mathfrak{E}(P_{a-j})(k) = \max\left(CH_{a-j}(k, k+\Delta l)\right) \\ \mathfrak{E}(P_{a-j+1})(k) = \max\left(CH_{a-j+1}(k, k+\Delta l)\right) \\ \mathfrak{E}(P_{b-j})(k) = \max\left(CH_{b-j}(k, k+\Delta l)\right) \\ \mathfrak{E}(P_{b-j+1})(k) = \max\left(CH_{b-j+1}(k, k+\Delta l)\right) \end{cases}, \quad k = 1,2,\cdots, L_1 - \Delta l \tag{8}$$

where CH_{a-j} is the data segment corresponding to time interval t_j of the signal collected by the sensor on P_a.

When nodes Pa and Pb are in different time intervals, the C-EWSD between P_a and P_b requires to calculate: the EWSD of CH_{a-j} and CH_{b-j+1} when the vehicle passes nodes P_a and P_b, the EWSD of CH_{a-j} and CH_{b-j} from two sensors corresponding to t_j, the EWSD of CH_{a-j+1} and CH_{b-j+1} from two sensors corresponding to t_{j+1}:

$$W'_{a-b} = \frac{1}{L_1 - \Delta l}\sum_{1}^{L_1-\Delta n}\left|\mathfrak{E}(P_{a-j}) - \mathfrak{E}(P_{b-j+1})\right| \tag{9}$$

$$W_{a-b}^{j} = \frac{1}{L_1 - \Delta l}\sum_{1}^{L_1-\Delta n}\left|\mathfrak{E}(P_{a-j}) - \mathfrak{E}(P_{b-j})\right| \tag{10}$$

$$W_{a-b}^{j+1} = \frac{1}{L_1 - \Delta l} \sum_1^{L_1 - \Delta n} \left| \mathfrak{E}\left(P_{a-j+1}\right) - \mathfrak{E}\left(P_{b-j+1}\right) \right| \quad (11)$$

The C-EWSD between nodes Pa and Pb in the adjacent time intervals is defined as:

$$W_{a-b} = \rho * W'_{a-b} + \sigma * W_{a-b}^{j} + \tau * W_{a-b}^{j+1} \quad (12)$$

2.3. Spatio-temporal graph construction based on data feature fusion

Graph learning extends the traditional single-node analysis to an intelligent diagnostic system with multi-source information fusion. The graph signal model is established rely on the "Node-Edge-Neighbors" system, which can be used to establish a system-level intelligent diagnostic system for structural health monitoring. In the " Node-Edge-Neighbor " relationship, the " Node " represents the sample object, the "Edge" is the relationship between the node and the proximity of the node, the "Neighbors" is the mutual adjacency of nodes. The length or diameter of the edge represents the weight of the relationship between the two neighboring points. The edges of directed graph have directionality. In this paper, we propose a data fusion algorithm to construct a spatio-temporal graph based on vibration signals. By fusing SDEW feature and other time-frequency features to build the weight between nodes. The node coordinates of the graph are updated according to the weight information and the original 3D coordinates. The location of defects can be determined from the node offsets effectively.

In this study, the graph structure is defined as:

$$\mathcal{G} = (V, E, A) \quad (13)$$

where $V \in R^{m \times 4}$ is the point set, including the node set and 3D coordinate of m nodes, the diagonal matrix $E \in R^{m \times m}$ is the edge set, containing the association and distance information, and A is the neighbor set, containing the neighborhood information of each node.

Bridge is a fixed structure, the neighbor set A is fixed. The point set V and edge set E change in the iterative calculation. The specific calculation steps are:

(1) Select SDEW and time-frequency features to calculate the correlation weight between nodes:

We designed a self-weighting analysis algorithm to measure the correlation between nodes (Li et al., 2021). Five sensitive features were selected from 13 time-domain metrics, 11 frequency-domain metrics, and 15 statistical-domain metrics, which were used to build the feature matrix Q_{a-b}:

$$Q_{a-b} = [W_{a-b}, W_{rms}, W_{per}, W_{pha}, W_{psd}, W_{cos}] \quad (14)$$

Where W_{a-b} is the proposed C-EWSD, the five sensitive features are Root Mean Square (W_{rms}), Pearson's Correlation coefficient (W_{per}), Phase correlation (W_{pha}), Power Spectral Density (W_{psd})and Spectral Cosine Similarity (W_{cos}). Among them, $W_{rms}$and W_{psd} are inverse indicators, and the other three are positive indicators.

(2) Normalization

Calculate the weight coefficient Q of the node based on the feature matrix Q_{a-b}:

$$Q_{a-b} = Q_{a-b} * \mathcal{R}^T \quad (15)$$

$$Q = \begin{bmatrix} Q_{1-1} & \cdots & Q_{1-m} \\ \vdots & \ddots & \vdots \\ Q_{m-1} & \cdots & Q_{m-m} \end{bmatrix} \quad (16)$$

where $\mathcal{R}^T$ is coefficient matrix.

Convert weights to distance multipliers Q_d between nodes and normalize:

$$Q_d = \frac{Q*2}{\max(Q)+\min(Q)} \quad (17)$$

(3) Spatio-temporal graph node update

The updated edge set E' is established based on the initial node edge set E:

$$E = \begin{bmatrix} d_{11} & \cdots & d_{1m} \\ \vdots & \ddots & \vdots \\ d_{m1} & \cdots & d_{mm} \end{bmatrix} \quad (18)$$

$$E' = E * Q^T \quad (19)$$

The spatio-temporal graph signals in different health states can be drawn through matrices E and E'. Changes in the distance between nodes can provide early warning of node damage information on the graph.

3. Experimental verification

The experimental device used in the paper is shown in Figure 4. The experimental device simulates the operation system of a two-section continuously supported highway steel truss bridge. The experimental setup consists of three reinforced concrete abutments, two steel truss bridges, a vehicle start-stop buffer section, and several vehicles, which can simulate a complete vehicle-bridge operation system. In this experiment, 8-channel vibration signal data sets were recorded under three health conditions, recorded as S_1 (normal), S_2 (P8-P14 truss fracture), and S_3 (P6-P12 truss fracture).

Fig. 4. Experimental truss bridge.

In this experiment, the S_1 and S_2 will be compared. When the truss between two nodes is damaged, the correlation and transitivity between the signals collected by the nodes at both ends of the truss will change. In this article, feature extraction is used to calculate this correlation or transitivity change. A spatio-temporal graph in two health states is established based on different feature relationships, and the fault location is determined based on the node distance on the graph.

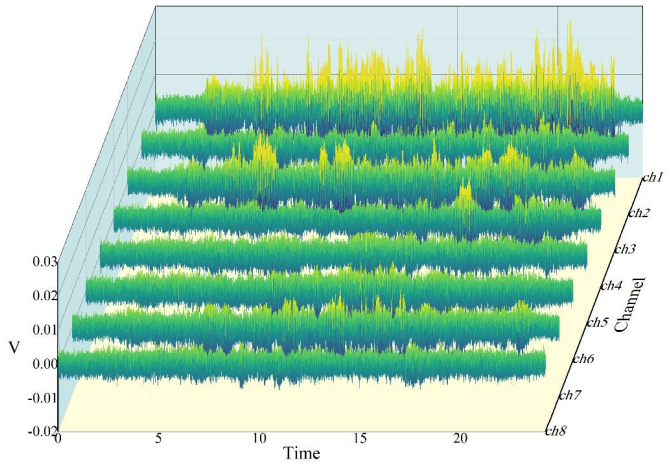

Fig. 5. 8-channel sensor monitoring data.

The 8-node vibration signal monitored using an 8-channel sensor is shown in Fig 5. The signal is segmented and dimensionally reduced according to the method proposed in this article. The extracted C-EWSD feature in the two health states are shown in Fig 6. It can be seen from the figure that when the truss at positions P8-P14 suffers from fracture damage, the C-EWSD feature metric on P8-P13, P8-P14, P8-P15 change significantly. Therefore, it can be preliminarily judged that the correlation between the signal at positions P8-P13, P8-P14, P8-P15 is reduced, and the faulty truss is related to position P8.

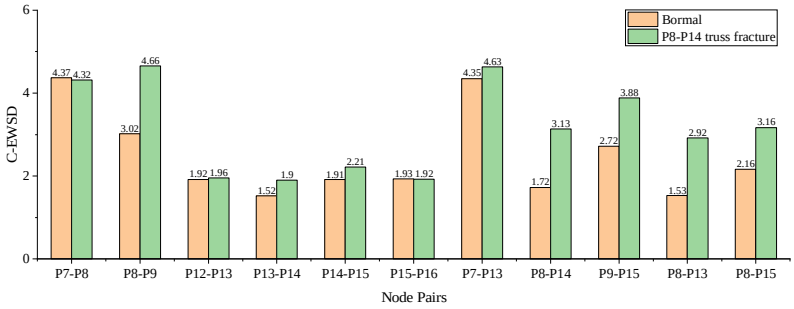

Fig. 6. Comparison of data C-EWSD features for two health states.

The sensitive features of the signal are further extracted for feature fusion. The feature matrix of S_2 is shown in Table 1. Calculate the association weights Q_{normal} and $Q_{P8-P14\ fracture}$ based on the fused features. After normalization, the node set is updated, the spatio-temporal graph and distance matrix in the two health states are obtained, as shown in Figure 7.

Table 1. Feature matrix of S_2 data.

Associated node pairs	C-EWSD	W_{rms}	W_{per}	W_{pha}	W_{psd}	W_{cos}
P7-P8	0.0043	0.0123	0.2013	0.3115	0.5931	0.6651
P7-P13	0.0046	0.01	0.2307	0.0633	0.6730	0.8146
P8-P9	0.0047	0.0131	0.3433	0.1336	0.5464	0.7423
P8-P13	0.0029	0.0113	0.4172	0.2597	0.8186	0.8735
P8-P14	0.0031	0.0084	0.3043	0.1553	0.8893	0.9028
P8-P15	0.0032	0.0099	0.2678	0.33	0.7823	0.8909
P9-P15	0.0039	0.0067	0.0858	0.7176	0.7407	0.6855
P12-P13	0.0020	0.0088	0.1132	0.017	0.0498	0.8142
P13-P14	0.0019	0.0051	0.1146	0.1119	0.8841	0.9120
P14-P15	0.0022	0.0052	0.0389	0.0597	0.8749	0.8954
P15-P16	0.0019	0.0102	0.5918	0.1969	0.9086	0.9076

The node P8 on the bridge is close to the five directly adjacent nodes (P7, P9, P13, P14, P15), especially the nodes P7 and P14 in Figure 7 (a). When the P8-P14 main truss breaks, the distance between the two nodes on the graph obviously increases. On the contrary, the data correlation with P13 and P15 has been strengthened. From the physical structure point of view, the P8 node is located on the upper layer of the bridge deck and is connected to the three bridge deck nodes P13, P14, and P15 through trusses. In the healthy state, node P14 is closest to P8 and has the strongest correlation. When the main trusses P8-P14 break, the truss structure of P8 and the bridge deck changes, and the original three truss connections are reduced to two. This directly leads to the transformation of the super-statically determinate structure between the four nodes P8, P13, P14, and P15 into a statically determinate structure. Therefore, the correlation between P8-P13 and P8-P15 is enhanced. However, P14 and P8 are no longer directly related but need to pass the correlation through other nodes such as P13 and P15. There is a significant decrease in the correlation of the analysis of vibration signals monitored from P8 and P14. From the data analysis, it can be effectively determined that there is an obvious failure in the P8-P14 main truss.

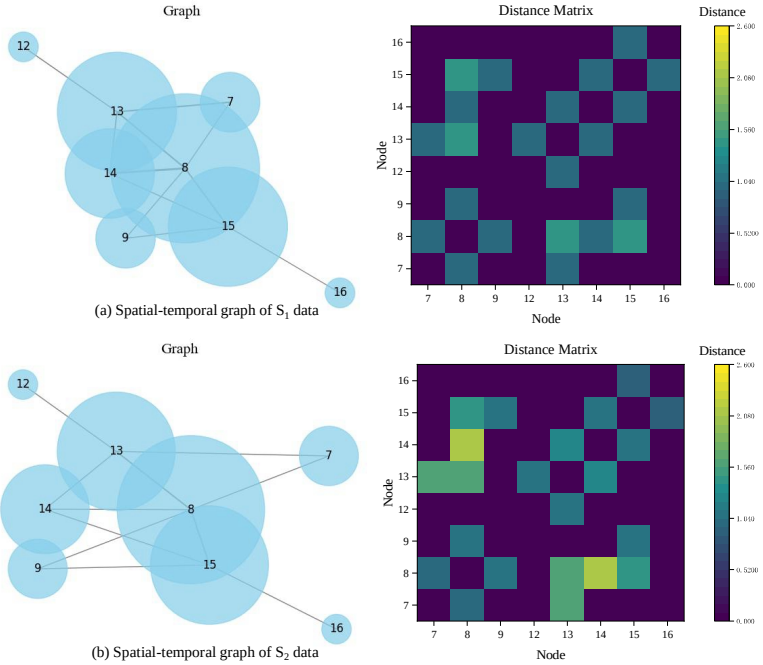

Fig. 7. (a) Spatio-temporal graph in normal state; (b) Spatio-temporal graph of P8-P14 truss fracture.

4. Conclusion

This paper proposes a spatio-temporal graph construction method based on vibration signals to study damage location and health monitoring of truss bridges. The C-EWSD feature extraction algorithm based on vibration signals is proposed to establish a correlation index between monitoring nodes. C-EWSD is used to fuse time-frequency sensitive features to develop a comprehensive evaluation index of the correlation between nodes. Based on the spatio-temporal signals monitored by multi-channel sensors, the spatio-temporal graph relationship between nodes is established. We built a truss bridge structural health monitoring test bench to perform data verification. The location of the fault can be effectively determined based on changes in distance between nodes. After data verification under different health states, this algorithm can effectively determine the fault location information of the truss bridge.

In future research, we will integrate multi-dimensional data and add different node combination information to comprehensively monitor the bridge status. At the same time, we use data dimensionality reduction algorithms to analyze the correlation and key nodes of sensor data to reduce the number of data collection channels. The most important thing is that we will establish a three-dimensional spatio-temporal graph signal from the monitoring data to more clearly judge the health status of the truss bridge.

Acknowledgements

This work was supported by the National Natural Science Foundation of China (52275079), the Youth Beijing Scholars program, the Guangxi Science and Technology Major Project (AA23062031), the BUCEA Doctor Graduate Scientific Research Ability Improvement Project, China.

References

Bao, Y., Beck, J. L., Li, H. 2011. Compressive sampling for accelerometer signals in structural health monitoring. Structural Health Monitoring 10(3), 235-246.

Bao, Y., Shi, Z., Wang, X., Li, H. 2018. Compressive sensing of wireless sensors based on group sparse optimization for structural health monitoring. Structural Health Monitoring 17(4), 823-836.
Delgadillo, R., Casas, J. 2019. Shm of bridges by improved complete ensemble empirical mode decomposition with adaptive noise (ICEEMDAN) and clustering. Enabling Intelligent Life-cycle Health Management for Industry Internet of Things (IIOT). Proceedings of IWSHM; 2019, 2111-2118.
Fischer, A., Igel, C. 2010. Empirical analysis of the divergence of Gibbs sampling based learning algorithms for restricted Boltzmann machines. In International conference on artificial neural networks (pp. 208-217). Berlin, Heidelberg: Springer Berlin Heidelberg.
Kim, C. W., Chang, K. C., Kitauchi, S., McGetrick, P. J., Hashimoto, K., Sugiura, K. 2014. Changes in modal parameters of a steel truss bridge due to artificial damage. In Proceedings of the 11th International Conference on Structural Safety and Reliability,(ICOSSAR) (pp. 3725-3732).
Li, L., Dong, F., Zhang, S. 2023. Adaptive spatio-temporal feature extraction and analysis for horizontal gas-water two-phase flow state prediction. Chemical Engineering Science 268, 118434.
Li, M., Wang, Y., Chen, Z., Zhao, J. 2021. Intelligent fault diagnosis for rotating machinery based on potential energy feature and adaptive transfer affinity propagation clustering. Measurement Science and Technology 32(9), 094012.
Li, S., Wei, S., Bao, Y., Li, H. 2018. Condition assessment of cables by pattern recognition of vehicle-induced cable tension ratio. Engineering Structures 155, 1-15.
Liu, Q. C., Wang, H. P. B. 2001. A case study on multisensor data fusion for imbalance diagnosis of rotating machinery. Ai Edam 15(3), 203-210.
Liu, Y., Cheng, M. M., Hu, X., Wang, K., Bai, X. 2017. Richer convolutional features for edge detection. In Proceedings of the IEEE conference on computer vision and pattern recognition, 3000-3009.
Mei, J., Moura, J. M. 2016. Signal processing on graphs: Causal modeling of unstructured data. IEEE Transactions on Signal Processing 65(8), 2077-2092.
Ortega, A., Frossard, P., Kovačević, J., Moura, J. M., Vandergheynst, P. 2018. Graph signal processing: Overview, challenges, and applications. Proceedings of the IEEE 106(5), 808-828.
Sandryhaila, A., Moura, J. M. 2013. Discrete signal processing on graphs. IEEE transactions on signal processing 61(7), 1644-1656.
Sandryhaila, A., Moura, J. M. 2014. Big data analysis with signal processing on graphs: Representation and processing of massive data sets with irregular structure. IEEE signal processing magazine 31(5), 80-90.
Song, M., Zhang, Z., Xiao, S., Xiong, Z., Li, M. 2022. Bearing fault diagnosis method using a spatio-temporal neural network based on feature transfer learning. Measurement Science and Technology 34(1), 015119.
Wei, S., Zhang, Z., Li, S., Li, H. 2017. Strain features and condition assessment of orthotropic steel deck cable-supported bridges subjected to vehicle loads by using dense FBG strain sensors. Smart Materials and Structures 26(10), 104007.
Xu, Y., Bao, Y., Chen, J., Zuo, W., Li, H. 2019. Surface fatigue crack identification in steel box girder of bridges by a deep fusion convolutional neural network based on consumer-grade camera images. Structural Health Monitoring 18(3), 653-674.
Xu, Y., Li, S., Zhang, D., Jin, Y., Zhang, F., Li, N., Li, H. 2018. Identification framework for cracks on a steel structure surface by a restricted Boltzmann machines algorithm based on consumer‐grade camera images. Structural Control and Health Monitoring 25(2), e2075.
Zhang, Q., Huang, C., Xia, L., Wang, Z., Yiu, S. M., Han, R. 2023. Spatial-temporal graph learning with adversarial contrastive adaptation. In International Conference on Machine Learning (pp. 41151-41163). PMLR.
Zhou, Z., Huang, Q., Wang, B., Hou, J., Yang, K., Liang, Y., Wang, Y. 2024. ComS2T: A complementary spatiotemporal learning system for data-adaptive model evolution. arXiv preprint arXiv, 2403.01738.